High-Resolution DNA Copy Number Profiling of Malignant Peripheral Nerve Sheath Tumors Using Targeted Microarray-Based Comparative Genomic Hybridization

Kiran K. Mantripragada,[1] Gillian Spurlock,[1] Lan Kluwe,[2] Nadia Chuzhanova,[3] Rosalie E. Ferner,[4] Ian M. Frayling,[5] Jan P. Dumanski,[6] Abhijit Guha,[7] Victor Mautner,[2] and Meena Upadhyaya[1,5]

Abstract

Purpose: Neurofibromatosis type 1 (NF1) is an autosomal dominant condition that predisposes to benign and malignant tumors. The lifetime risk of a malignant peripheral nerve sheath tumor (MPNST) in NF1 is ~10%. These tumors have a poor survival rate and their molecular basis remains unclear. We report the first comprehensive investigation of DNA copy number across multitude of genes in NF1 tumors using high-resolution array comparative genomic hybridization (CGH), with the aim to identify molecular signatures that delineate malignant from benign NF1 tumors.

Experimental Design: We constructed an exon-level resolution microarray encompassing 57 selected genes and profiled DNA from 35 MPNSTs, 16 plexiform, and 8 dermal neurofibromas. Bioinformatic analysis was done on array CGH data to identify concurrent aberrations in malignant tumors.

Results: The array CGH profiles of MPNSTs and neurofibromas were markedly different. A number of MPNST-specific alterations were identified, including amplifications of *ITGB4, PDGFRA, MET, TP73*, and *HGF* plus deletions in *NF1, HMMR/RHAMM, MMP13, L1CAM2, p16INK4A/CDKN2A*, and *TP53*. Copy number changes of *HMMR/RHAMM, MMP13, p16INK4A/CDKN2A*, and *ITGB4* were observed in 46%, 43%, 39%, and 32%, respectively of the malignant tumors, implicating these genes in MPNST pathogenesis. Concomitant amplifications of *HGF, MET*, and *PDGFRA* genes were also revealed in MPNSTs, suggesting the putative role of p70S6K pathway in NF1 tumor progression.

Conclusions: This study highlights the potential of array CGH in identifying novel diagnostic markers for MPNSTs.

Neurofibromatosis type 1 (NF1; OMIM # 162200) is a common autosomal dominant disorder with a prevalence of 1 in 3,000 individuals worldwide. The majority of individuals with NF1 develop benign dermal neurofibromas, and approximately one third have benign plexiform neurofibromas (1, 2). In 5% to 10% of NF1 patients, neurofibromas (predominantly plexiform) develop into malignant peripheral nerve sheath tumors (MPNST; ref. 3). Whereas approximately half of all MPNSTs in the general population occur in the context of NF1, the other 50% are sporadic in origin. To date, understanding of histogenesis and the molecular mechanisms leading to the malignancy in NF1 remains fragmentary.

The loss of neurofibromin, the protein product of the *NF1* gene, has been documented in sporadic and NF1-associated MPNSTs (4). Altered expression of the *TP53*, *RB1*, *p16INK4A/CDKN2A*, *p14/ARF*, *p27/KIP1*, and *EGFR* genes have also been identified exclusively in malignant tumors (1, 5, 6). These studies suggest that loss of neurofibromin is the primary event for tumor initiation, whereas additional genetic lesions are required for progression to malignancy.

A number of studies have attempted to identify molecular signatures that can differentiate between MPNSTs and benign neurofibromas. The majority of these studies have analyzed gene expression patterns (1, 5, 7–14), and a few studies have reported analysis of deletions and amplifications (15–18). However, the DNA dosage studies were generally limited by the low resolution of analysis and/or because of the small number of genes analyzed. It is now known that gene copy number and expression levels correlate with each other, and that it is possible to identify patterns of gene deletions and

Authors' Affiliations: [1]Institute of Medical Genetics, Cardiff University, School of Medicine, Heath Park, Cardiff, United Kingdom; [2]Department of Neurosurgery, University Clinic Hamburg-Eppendorf, Hamburg, Germany; [3]Department of Biological Sciences, University of Central Lancashire, Preston, United Kingdom; [4]Department of Clinical Neurosciences, Guy's, King's and St. Thomas' School of Medicine, London Bridge, London, United Kingdom; [5]University Hospital of Wales College of Medicine, Heath Park, Cardiff, United Kingdom; [6]Department of Genetics, University of Alabama at Birmingham, Medical School, Birmingham, Alabama; and [7]The Arthur and Sonia Labatt Brain Tumor Research Centre, The Hospital for Sick Children, University of Toronto, Toronto, Ontario, Canada

Received 5/29/07; revised 10/23/07; accepted 10/25/07.

Grant support: Cancer Research UK, United States Department of Defense no. W81XWH0610280, and German Cancer Foundation no. 107047.

The costs of publication of this article were defrayed in part by the payment of page charges. This article must therefore be hereby marked *advertisement* in accordance with 18 U.S.C. Section 1734 solely to indicate this fact.

Note: Supplementary data for this article are available at Clinical Cancer Research Online (http://clincancerres.aacrjournals.org/).

Requests for reprints: Kiran K. Mantripragada, Institute of Medical Genetics, Cardiff University, School of Medicine, Heath Park, Cardiff, United Kingdom, CF14 4XN. Phone: 0044-29-20744079; E-mail: kiran.mantripragada@gmail.com.

doi:10.1158/1078-0432.CCR-07-1305

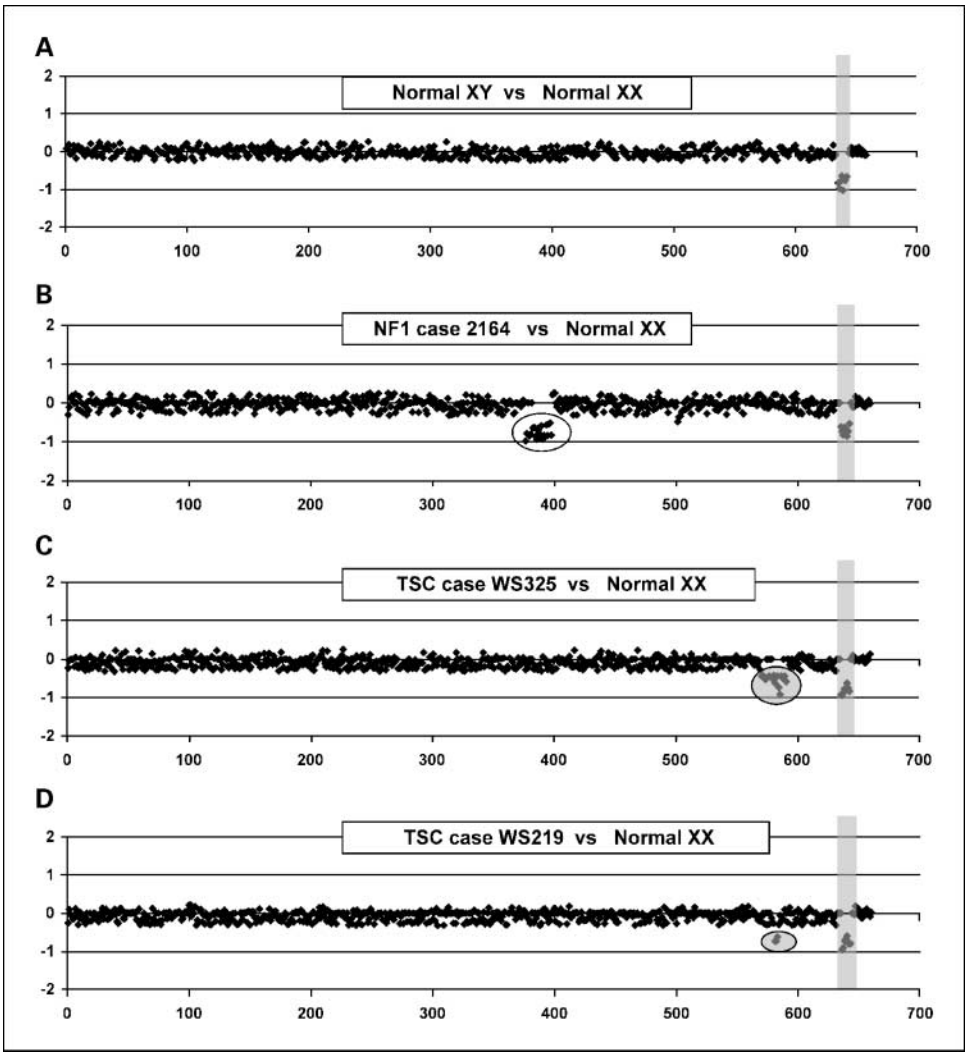

Fig. 1. Validation of the MPNST microarray. *X*-axis, measurement points on the microarray; *Y*-axis, $\log_2$ value of the average normalized ratio of fluorescence. All array CGH profiles will follow the above-mentioned description. *A,* array CGH profile for the hybridization of a normal male (*XY*) to normal female DNA (*XX*). As expected, the autosomal control loci (ID 642-656) displayed fluorescence ratios for two copies (0.00 ± 0.07; ratio ± SD); and the chromosome X loci (*shaded column*; ID 634-641) showed fluorescence values for one copy (-0.80 ± 0.10). The normalized ratios of fluorescence for all the 57 selected genes (ID 1-633) were consistent with diploid copies (-0.02 ± 0.11). *B,* identification of the previously characterized total *NF1* gene deletion in male patient 2164. The normalized ratio for the *NF1* gene (ID 376-398), highlighted in the oval, was -0.76 ± 0.10 consistent with one gene copy. *C,* detection of the previously known total *TSC2* gene deletion in male patient WS325. The *TSC2* gene on the array (ID 571-591) displayed normalized ratios (-0.53 ± 0.13) indicating one gene copy. *D,* array CGH profile of a previously characterized male TSC case WS219, which contains deletion of exons 29 and 30 in the *TSC2* gene. Three data points that span the *TSC2* exons 29 and 30 (ID 581-583) showed fluorescence ratios for one gene copy (-0.73 ± 0.01).

amplifications that are specific to benign, premalignant, and malignant states (19, 20).

In this work, we selected 57 genes that were relevant in MPNST development and profiled their DNA copy number changes in malignant and benign NF1 tumors using microarray-based comparative genomic hybridization (array CGH). This is the first high-resolution study of DNA dosage across a multitude of genes in a large number of NF1 tumors. We show a high frequency of MPNST-specific alterations in *HMMR/RHAMM*, matrix metalloproteinase-13 (*MMP13*), *p16INK4A/CDKN2A*, integrin β-4 (*ITGB4*), *HGF*, *MET*, and *PDGFRA* genes, which advocates the putative role of these genes and their related biological pathways in the initiation and/or progression of MPNSTs.

Materials and Methods

Patient material. The samples included in this study were provided by genetic centers from the United Kingdom (Cardiff and London), Germany (Hamburg), and Canada (Toronto). The study was ethically approved by the relevant institutional research boards in each center. DNA derived from 59 tumor samples from 55 NF1 patients (Supplementary Table S1), including 35 MPNSTs, 16 plexiform, and 8 dermal neurofibromas were studied. Matched constitutional lymphocyte DNA from 10 MPNSTs (Supplementary Table S1) were also hybridized. In addition, for validation studies, three previously characterized DNA samples were profiled, including NF1 case 2164 that is known to have a complete *NF1* gene deletion, and tuberous sclerosis 2 (TSC2) cases WS325 and WS219 that contain a complete and partial deletion of the *TSC2* gene, respectively.

Construction of the microarray. The array was constructed using a previously reported PCR-based approach for microarrays production (21, 22). Briefly, genomic sequences from the 57 selected genes (Supplementary Table S2) were downloaded from Ensembl[8] (human genome build 35.1), and bioinformatic analysis was carried out using Sequence Allocator program.[9] The program combines and automates filtering out redundant stretches in the input genomic sequence and designing primers in the unique fragments.

For 57 selected genes, 633 primer pairs (ID 1-633) were selected, which mainly covered the exonic sequences. In addition, 8 loci from chromosome-X (ID 634-641) and 15 autosomal control loci (ID 642-656) were also included in the construction of the microarray. The

[8] http://www.ensembl.org
[9] http://puffer.genpat.uu.se

Table 1. Details ot DNA copy number alterations in MPNST samples

SI. No	Sample	Grade	Deleted genes	Amplified genes
1	M-1	Intermediate	*FABP7, HMMR, HSPCA, MMP13, NF1,p16-INK4a,**	*BIRC5, CCNE2, CMA1, CCND1, EGFR, FLT4, HGF, ITGB4, MET, MMP9, PDGFRA, SPP1, TERT, TP73, TSC2*
2	M-2	High	*HMMR, NF1, p16-INK4a**	*CCNE2, HGF, ITGB4, MET, MMP9, PDGFRA, SPP1, TERT, TP73*
3	M-3	Unknown	*HMMR, L1CAM2*	*CCND1, RASSF2*
4	M-4	Intermediate	*FABP7, HMMR, L1CAM2, MMP13, NF1, p16-INK4a*	*BIRC5, CCNE2, CMA1, EGFR, HGF, ITGB4, MET, PDGFRA, SPP1, TERT, TP73*
5	M-5	Intermediate	*HGF, HMMR, MET, NF1,OSF2, p16-INK4a, RASSF2, RB1, TNFRSF10A TP53 EGFR*	
6	M-6	Unknown	*FABP7, L1CAM2, MKi-67, mTOR, NF1, p16-INK4a*, PTCH2, PTEN, RASSF2, TIMP4*	*BIRC5*
7	M-7	High	*HGF, HMMR HSPCA, L1CAM2, MET, NF1, OSF2, p16-INK4a, RASSF2, RB1*	*EGFR, ITGB4, MMP9*
8	M-8	High	*HMMR, L1CAM2, MMP13, NF1, PTEN, RB1, TP53*	*CCNE2, CCND1, EGFR, ERBB3, IL8, PDGFRA, SOX10*
9	M-9	High	*L1CAM2, NF1, p16-INK4a*	*BIRC5, CCNE2, CCND1, EGFR, FLT4, FOS, FOXA2, HGF, ITGB4, MET, PDGFRA, SOX10, TERT, TGFB1, TP73, TSC1*
10	M-10	High	*L1CAM2, MMP13, mTOR, NF1, OSF2, p16-INK4a, PTCH2, RASSF2, RB1*	*MDM4, MPZ*
11	M-11	Low	*NF1,† OSF2, RB1, TOP2A*	*CDKN1A, CCND1, FLT4, FOXA2, Gl1, ITGB4, SOX10, TERT, TGFB1, TP73, TSC2*
12	M-12	Low	—	—
13	M-13	High (Triton)	*HMMR, MMP13, mTOR, NF1, OSF2, p16-INK4a, PTCH2, RB1, TP53*	*CCNE2, SOX10, TOP2A*
14	M-14	Unknown	*FABP7, HMMR, HSPCA, Mki-67, MMP13, NF1,‡ p16-INK4a, PTEN, TP53*	*BIRC5, CCND1, EGFR, ITGB4, TERT, TOP2A*
15	M-15	Low	—	*mTOR*
16	M-16	High	*MMP13, NF1*	*BIRC5, ITGB4, MPZ, RASSF2, TSC2*
17	M-17	Low	*NF1,† TOP2A*	*FOXA2*
18	M-18	High	—	*BIRC5, CCNE2, HGF, MET, PDGFRA*
19	M-19	High	*NF1*	*CCND1, ITGB4, MMP9, PTCH2, SOX10, TERT, TP73, TSC2*
20	M-20	High	*EPHA7, FN1, HMMR, Mki-67, MMP13, NF1, P16-INK4a, RB1*	*BIRC5, ITGB4, TERT*
21	M-21	High	*Mki-67, mTOR, NF1, PTEN, SPP1*	*HGF, MDM4, MET, MPZ, PDGFRA*
22	M-22	High	*FABP7, EPHA7, MKi-67, MMP13, RASSF2*	*TOP2A*
23	M-23	High	*HMMR, MMP13, NF1, RASSF2, TP53*	—
24	M-24	High	—	—
25	M-25	High	*HMMR, HSPCA, Mki-67, MMP13, NF1, SPP1*	—
26	M-26	High	*HMMR, HSPCA, L1CAM2, MMP13, NF1, RASSF2*	*mTOR*
27	M-27	High	*L1CAM2,† RASSF2, RB*	—
28	M-28	High	—	—
29	M-29	Unknown	—	—
30	M-30	Unknown	*MMP13, NF1, RASSF2, TP53*	*BIRC5, CCNE2, CCND1, EGFR, FLT4, FOXA2, HGF, HSPCA, ITGB4, MDM4, MET, MTOR, PDGFRA, S100B, TERT, TOP2A, TP73*
31	M-31	Unknown	*FABP7, HMMR, MMP13, NF1, OSF2, p16-INK4a, RB1*	*CDKN1B/p27, FLT4, FOXM1, RASSF2*
32	M-32	Unknown	*FN1, NF1, p16-INK4a, TOP2A*	*BIRC5, CCND1, ITGB4*
33	M-33	Unknown	*HMMR, L1CAM2, SPP1*	*ITGB4*
34	M-34	Unknown	*FABP7, EPHA7, MMP13, p16-INK4a, RB1, TNFRSF10A, TNFRSF10B*	*FLT4, L1CAM2, SOX10*
35	M-35	Unknown	*CCNE2, HMMR, HSPCA†*	*OSF2*

*Homozygous deletion.
† Partial deletion of the gene.
‡ Partial homozygous deletion.

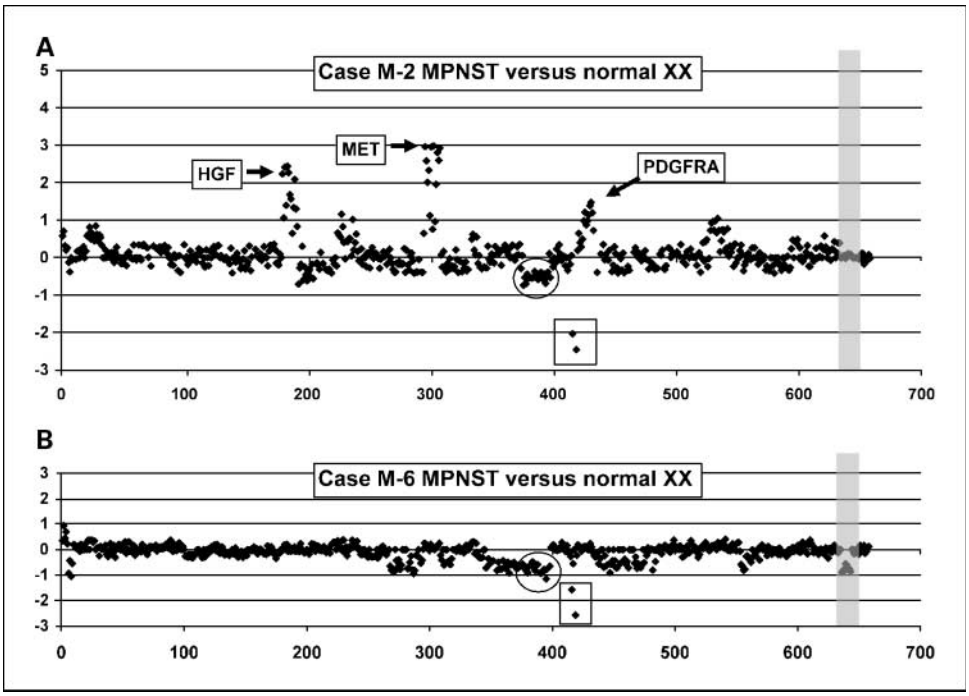

Fig. 2. Application of the MPNST array for array CGH profiling of malignant and benign tumors from NF1 patients. *A,* hybridization of the female MPNST case M-2 to the microarray identified high proportion of amplifications (Table 1). The prominent copy number gains in *HGF* (1.75 ± 1.37), *MET* (2.56 ± 1.93), and *PDGFRA* (0.99 ± 0.46) are indicated. Oval, hemizygous deletion of the *NF1* gene (-0.55 ± 0.03); rectangle, biallelic loss of *p16INK4A/CDKN2A* gene (ID 415 -420; -1.68 ± 0.16). *B,* array CGH analysis of male MPNST case M-6 shows predominance of deletions (Table 1). Oval, hemizygous deletion of the *NF1* gene (-0.76 ± 0.06); rectangle, biallelic loss of *p16INK4A/CDKN2A* gene (-1.36 ± 0.18).

sequence details of all primer pairs and product lengths are given in Supplementary Table S3. The PCR products ranged in size from 142 to 1,000 bp (average 727 bp). To obtain exon-level resolution of analysis, individual PCR products were suspended in spotting buffer [0.25 mol/L phosphate buffer (pH 8.5); 0.00025% sarkosyl] and spotted in triplicate on CodeLink slides (GE Healthcare).

Hybridization, scanning, and image analysis. The blocking of microarrays, hybridization, and prehybridization and posthybridization processing of the slides was done as previously reported (22). A pool of DNA derived from 20 normal and unrelated females was used as control DNA in the hybridization experiments. Image acquisition was done using the Agilent Scanner (Agilent Technologies) at 10 μm resolution, and image analysis was carried out using the BlueFuse software (BlueGnome Limited). The data were exported to MS Excel for further analysis. The average, SD, and coefficient of variance of the three replicas for each data point were calculated. Clones displaying a coefficient of variance that is >5% between a minimum of two replicate spots were discarded. The average ratio from the autosomal controls was used in the normalization of all measurement points on the array. For each data point, a $\log_2$ value of <-1.80 indicates a biallelic loss, -0.40 to -1.0 reflects a hemizygous deletion, and a value of >+0.40 is indicative of copy number gain. An alteration was considered to be positive only if two consecutive data points displayed a similar normalized ratio of fluorescence. Dye swap experiments were done for all samples that showed an alteration.

Multiplex ligation–dependent probe amplification analysis. The deletion status of the *NF1* gene was confirmed in 7 MPNSTs, 10 plexiform, and 1 dermal neurofibroma (Supplementary Table S1) using the multiples ligation–dependent probe amplification (MLPA) technique with the SALSA P081/082 NF1 MLPA kit (Medical Research Council Holland). Hybridization, ligation, and amplification of the MLPA probes were carried out as described (22).

Quantitative real-time PCR. Array CGH data for the relative DNA copy numbers of 10 genes (*CCND1*, *EGFR*, *HGF*, *HMMR/RHAMM*, *L1CAM2*, *MET*, *p16INK4A/CDKN2A*, *PDGFRA*, *RB1*, and *TERT*) were validated in 6 samples (M-2, M-4, M-5, M-8, M-9, and M-14) in triplicate measurements by quantitative PCR using a 7500 Real-Time PCR System (Applied Biosystems) and SYBR Green PCR master mix (Applied Biosystems). The *Ct* values were calculated by the absolute quantification method. The β-*actin* gene was used as gene reference and DNA from a normal female as reference DNA. Primers for gene amplification were designed using Primer Express (Applied Biosystems). The size of all products was 51 bp. The details of all genes and primers are given in Supplementary Table S4.

Bioinformatic analysis. The occurrence of each of the possible $\binom{N}{k} = \frac{N\times(N-1)\times\ldots\times(N-k+1)}{k!}$ combinations that can be made out of N genes by taking three (k = 3) and four (k = 4) genes at a time was calculated using purposely designed software. The genes found both deleted and amplified were considered as different genes; therefore, the total amount of genes N was set to 67. Combinations of three genes (k = 3) of N = 67 genes found in the data set with the frequency of ≥7 and present in 66% of the patients were chosen for the further investigation.

To assess the significance of our findings, 1,000 data sets comprising 35 random combinations of deleted and amplified genes matching the corresponding original sample in terms of the number of deleted and amplified genes were simulated.

Results

Validation of the cancer chip. The performance of the cancer chip was validated by four experiments (Fig. 1). The array CGH profile of the hybridization of normal male (XY) DNA against normal female (XX) DNA is shown in Fig. 1A. As expected, the $\log_2$ values of the average normalized ratios of fluorescence for all the autosomal control loci showed two copies, whereas the fluorescence ratios for the chromosome X loci indicated one DNA copy. Because all the 57 selected genes were of autosomal origin, their normalized ratios of fluorescence were consistent with two copies.

Constitutional DNA samples from three male patients with known mutations were used to further evaluate the sensitivity and specificity of the MPNST microarray. The array CGH analysis of DNA from the NF1 patient 2164 and the TSC2 case WS325 displayed normalized fluorescence ratios consistent

Table 2. List of most frequently aberrant genes in MPNSTs

Gene	% of MPNST cases displaying aberration	Copy number alteration
NF1	71	Deletion
HMMR/RHAMM	46	Deletion
MMP13	43	Deletion
p16-INK4a	39	Deletion
LICAM2	29	Deletion
RASSF2	25	Deletion
RB1	25	Deletion
ITGB4	32	Amplification
PDGFRA	29	Amplification
BIRC5	25	Amplification
CCNE2	25	Amplification
EGFR	25	Amplification
HGF	25	Amplification
MET	25	Amplification
TERT	25	Amplification

with hemizygous deletions of the *NF1* gene and the *TSC2* gene, respectively (Fig. 1B-C). For testing the performance of the array in detecting exonic deletions, we hybridized DNA from TSC2 case 219, which has been previously characterized to contain hemizygous deletion of the *TSC2* exons 29 and 30. Figure 1D displays the array CGH profile for this sample.

Application of the MPNST microarray. Gene dosage imbalances were detected in all but four MPNSTs (M-12, M-24, M-28, and M-29). In the remaining 31 cases (89%), DNA aberrations of the majority of the genes were observed, and the results are summarized in Table 1. A varied degree of gene copy number changes were observed in MPNSTs. One tumor (M-1) showed alterations in 21 genes, whereas another tumor (M-15) displayed alterations in only one gene. The level of copy number changes for the same gene varied greatly in different tumor samples. The copy number of the *MET* oncogene, for example, ranged from 2 copies to 16 copies in malignant tumors (Fig. 2). Also, we detected both partial and total gene deletions for the *HSPCA, L1CAM2*, and *NF1* genes in MPNSTs. In summary, we observed amplifications of 34 genes and deletions of 23 genes, including 10 genes that displayed both amplifications and deletions. There was no obvious correlation between the MPNST tumor grade and the copy number alterations (Table 2).

Loss of genetic material seems to be more frequent than amplifications in MPNSTs. Whereas 18 of 35 samples (51%) displayed predominant deletions, only 10 (29%) exhibited reciprocal profiles. Figure 2 displays the array CGH profiles of two representative MPNST cases. Deletions of the *NF1* gene were observed in all the three types of NF1 tumors (dermal and plexiform neurofibromas, and MPNST) analyzed in this study (Fig. 2; Table 1), which is a clear confirmation that mutation of the *NF1* gene is the primary event in NF1 tumorigenesis. In agreement with previous data (23, 24), deletion of the *NF1* gene was the most frequent aberration (71%) observed in the MPNST series.

In the MPNST M-14, we detected two levels of deletion in the *NF1* gene, including homozygous deletion of the *NF1* exons 2 and 3 and hemizygous loss of the remaining exons (Fig. 3A). Array CGH profiling of DNA from the dermal neurofibroma (D-14; Fig. 3B), plexiform (P-14; Fig. 3C), and

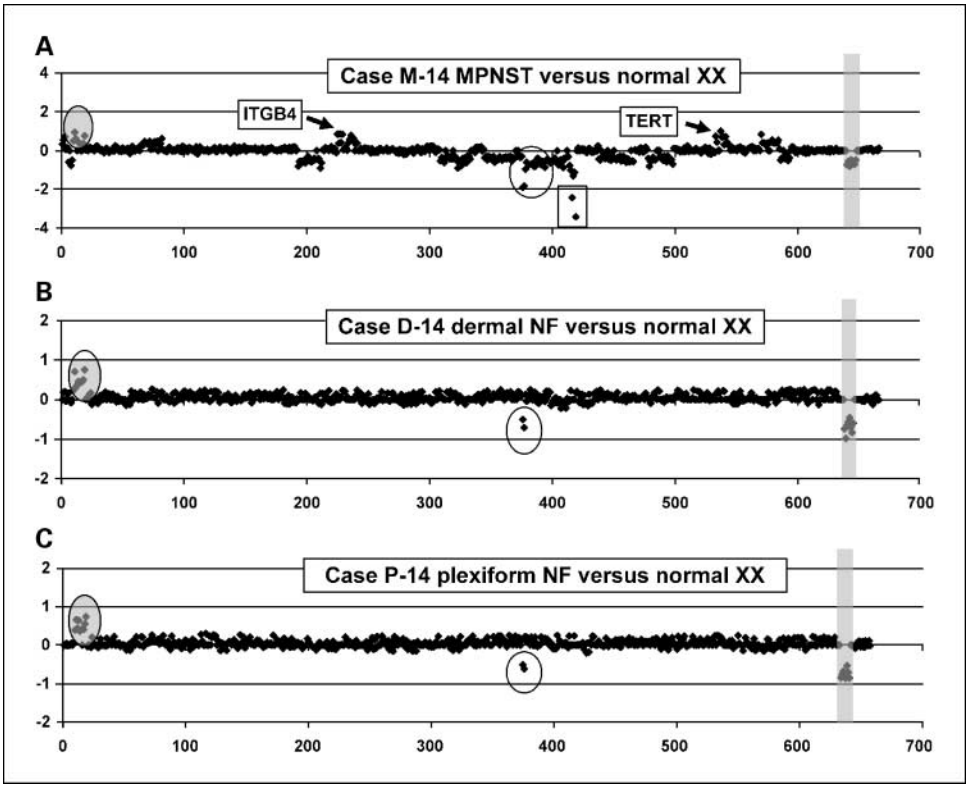

Fig. 3. Comparison of hybridization profiles of MPNST, dermal, and plexiform neurofibroma samples from the male patient 14. The germline mutation in this patient was the hemizygous deletion of the *NF1* exons 2 and 3. Shaded oval, amplification of the *CCND1* gene (ID 10-19). *A,* array CGH profile of MPNST sample M-14. Oval, homozygous deletion of the *NF1* exons 2 and 3 (ID 376 and 377; -1.85 $\pm$ 0.01) and the hemizygous loss of the remaining *NF1* gene (ID 378-398; -0.64 $\pm$ 0.06). Rectangle, biallelic loss of the *p16/INK4A/CDKN2A* gene (-1.80 $\pm$ 0.16). *B,* hybridization of the dermal neurofibroma sample D-14 and (*C*) the plexiform sample P-14 to the MPNST array identified the germline mutation and the amplification of the *CCND1* gene.

blood (B-14; data not shown) samples obtained from the same patient detected a one copy loss of the *NF1* exons 2 and 3, indicating that this deletion is the germline mutation in patient 14 (25). In two MPNST samples (M-11 and M-17), we detected partial hemizygous deletions of the *NF1* gene of identical size (26.1 kb) and span (ID 376-380; Fig. 4A). To validate these findings, we did MLPA on sample M-17, which detected the one-copy loss of exons 1 to 6 (Fig. 4B). These analyses establish the exon level resolution (3.1 kb) of the MPNST chip.

We identified deletions of the *HMMR*, *MMP13*, and *p16INK4A/CDKN2A* genes in 46%, 43%, and 39% of MPNSTs, respectively; whereas amplifications of *ITGB4* were seen in 32% of the malignant cases (Table 2). Moreover, the MPNST analysis revealed the occurrence of parallel DNA alterations in two genes encoding hepatocyte growth factor (*HGF*) and its functional receptor MET proto-oncogene (*MET*). Out of nine MPNST samples that displayed copy number imbalances for *HGF* and *MET*, seven cases (78%) showed coamplification, and two tumors (22%) displayed concomitant deletions. The colocalization of these genes on 7q might explain the coincidence of the alterations. It was also observed that amplifications but not deletions of the *HGF* and *MET* genes were accompanied by amplifications of the platelet-derived growth factor receptor, α (*PDGFRA*) gene. Table 2 lists the most frequently altered genes in MPNSTs using array CGH.

The analysis of DNA from benign plexiform and dermal neurofibromas showed that, apart from the specific lesions of the *NF1* gene, the only consistent alteration in these tumors was amplification of the cyclin D1 (*CCND1*) gene (3B-C), which was observed in 4 of 16 plexiforms (25%) and 1 of 8 dermal neurofibromas (12%). Hybridization of DNA derived from the constitutional tissue (blood) from 10 MPNST patients did not reveal copy number changes in any

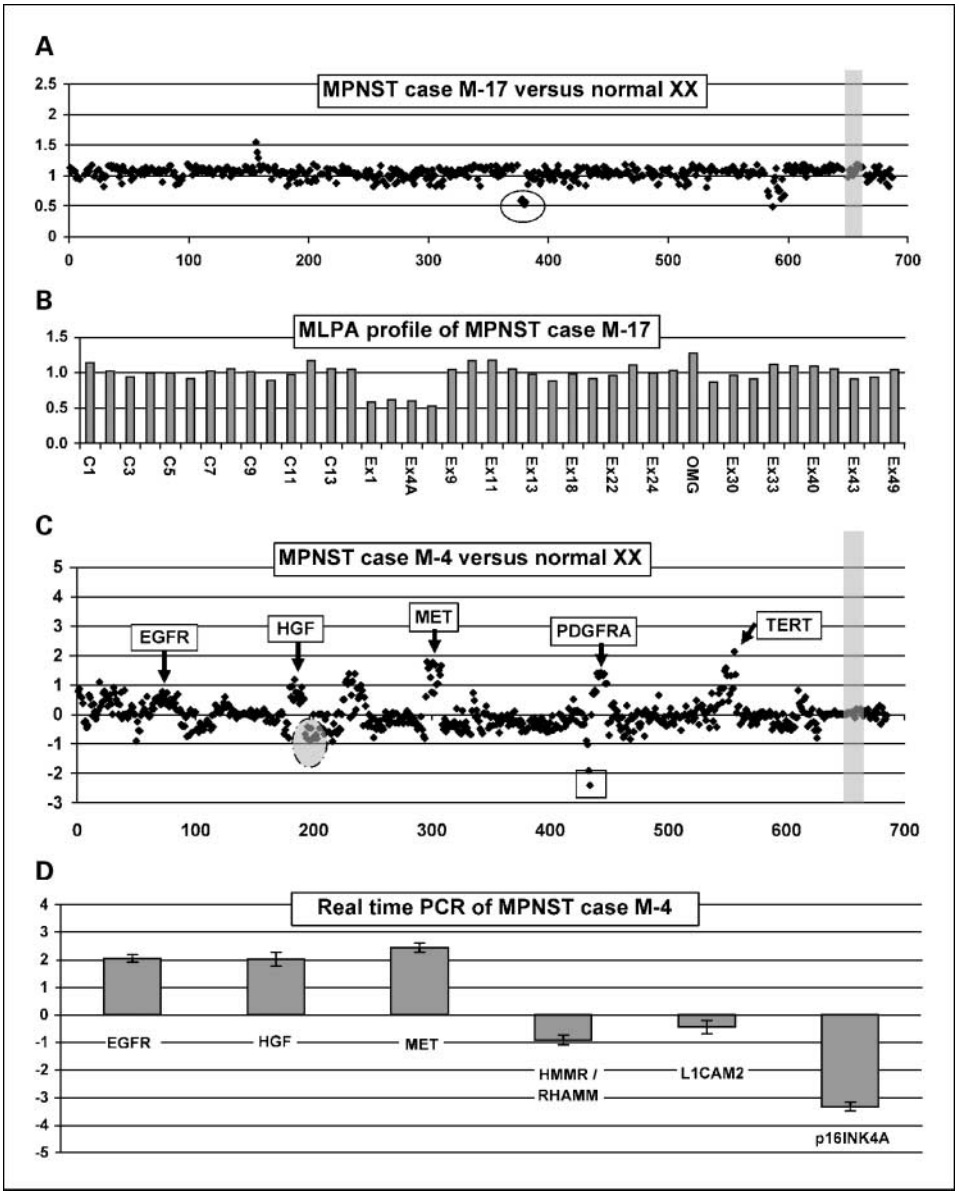

Fig. 4. Confirmation of array CGH data by MLPA and real-time PCR. *A,* array CGH profile of DNA derived from MPNST sample M-17. The intragenic deletion in the *NF1* gene was detected by five measurement points (ID 376-380; -0.83 ± 0.03) that span exons 2 through 7. *B,* the MLPA analysis of M-17 sample for DNA copy number alterations in the *NF1* gene revealed an intragenic deletion spanning exons 1 through 6 (0.58 ± 0.04). Probes C1-C14, autosomal control probes. *C,* array CGH analysis of MPNST case M-4. Shaded oval, one copy deletion of the *HMMR/RHAMM* gene (-0.66 ± 0.07); rectangle, biallelic loss of *p16INK4A/CDKN2A* gene (-1.64 ± 0.71). The copy number gains are indicated for *EGFR* (0.50 ± 0.10), *HGF* (0.74 ± 0.26), *MET* (1.5 ± 0.51), *PDGFRA* (1.26 ± 0.22), and *TERT* (0.65 ± 0.20) genes. *D,* validation of DNA copy number changes in MPNST case M-4 using real-time PCR. *Y*-axis, $\log_2$ ratios of gene copy number and the SD values across the triplicate measurements. The suboptimal level for deletion of the *L1CAM2* deletion by real-time PCR may be explained by the polyploid nature of the MPNST.

Table 3. Bioinformatic analysis of array CGH data from MPNST samples

A. Combinations of three deleted and/or amplified genes present in ≥7 MPNST samples including the *NF1* gene

Deleted genes			Amplified genes					Number of combinations
NF1	*HMMR*	*MMP13*						10
NF1	*HMMR*		*p16-INK4a*					9
NF1		*MMP13*	*p16-INK4a*					7
NF1			*p16-INK4a*	*BIRC5*				7
NF1			*p16-INK4a*					8
NF1				*BIRC5*	*ITGB4*			8
NF1					*ITGB4*	*CCND1*		7
NF1					*ITGB4*		*TERT*	9
NF1					*ITGB4*			*TP73* 7
NF1							*TERT*	*TP73* 7
					ITGB4		*TERT*	*TP73* 7
					HGF	*MET*	*PDGFRA*	7

B. Combinations of three deleted and/or amplified genes present in ≥6 MPNST samples excluding the NF1 gene

Deleted genes			Amplified genes				Number of combinations
				ITGB4	*TERT*	*CCND*	6
				ITGB4	*TERT*	*TP73*	7
			BIRC5	*ITGB4*	*TERT*		6
		p16-INK4a		*ITGB4*	*TERT*		6
		p16-INK4a	*BIRC5*	*ITGB4*			6
	MMP13		*BIRC5*	*ITGB4*			6
HMMR		*p16-INK4a*		*ITGB4*			6
HMMR	*MMP13*	*p16-INK4a*					6
			HGF	*MET*	*PDGFRA*		7
			HGF	*MET*		*CCNE2*	6
			HGF		*PDGFRA*	*CCNE2*	6
				MET	*PDGFRA*	*CCNE2*	6

of the 57 genes, with the exception of the NF1 gene deletion in patient 14.

Bioinformatic analysis. Bioinformatic analysis was done on the array CGH data to investigate the concurrence of gene copy number alterations in MPNSTs by comparison with a simulated data set. To identify the most significant combinatorial alterations, we chose a threshold of three genes (deleted and/or amplified) identified in at least seven MPNST samples (Table 3A). The most frequent combination included deletions of *NF1*, *HMMR*, and *MMP13* genes that occurred in 10 samples. We also analyzed the data by excluding the *NF1* gene and with the threshold of three altered genes present in ≥6 MPNST samples (Table 3B). There were two combinations that were most frequent, namely the amplification of *HGF-MET-PDGFRA* and *ITGB4-TERT-TP73* in seven samples each.

Ten genes, namely *CCNE2*, *HGF*, *L1CAM*, *MET*, *mTOR*, *OSF2*, *PTCH2*, *RASSF2*, *SPP1*, and *TOP2A* were found either to be deleted or amplified. Striking disproportion in the frequencies of the same genes being amplified and deleted in the case data set was observed for *CCNE2* (deleted in one sample and amplified in eight samples) and *L1CAM2* (deleted in 10 samples and amplified in 1) genes, whereas for 1,000 simulated data sets, the asymmetry is less pronounced (deleted in five and amplified in seven samples on average). Two-way ANOVA shows that the case and simulated data sets result in significantly different (P = 0.0029) mean number of samples in which deletion and amplification of these 10 genes were observed. A Spearman rank correlation coefficient was used to study correlations between the number of genes being deleted and amplified in the case and simulated data sets. A high negative correlation was noted between deleted and amplified genes in the case data set (r_s = -0.8744; one-tailed probability, P = 0.000465); no significant correlation was observed in the simulated data set (r_s = -0.1193; P = 0.3713).

Confirmation of array CGH data. MLPA was done in DNA samples from 7 MPNSTs, 10 plexiform, and 1 dermal neurofibroma (Supplementary Table S1). In these tumors, array CGH detected the *NF1* gene deletions in three MPNSTs, one plexiform, and one dermal neurofibroma. In all the cases, including intragenic deletions, there was agreement between the microarray and MLPA data (Fig. 4A-B), confirming the sensitivity and specificity of the array CGH technology. The copy number changes of 10 genes (*CCND1*, *EGFR*, *HGF*, *RHAMM*, *L1CAM2*, *MET*, *p16INK4A/CDKN2A*, *PDGFRA*, *RB1*, and *TERT*) detected in 6 MPNSTs were confirmed by quantitative real-time PCR. The array CGH and real-time data for case M-4 are shown in Fig. 4C-D. Amplifications in the *EGFR*, *HGF*, and *MET* genes; one copy loss of *HMMR/RHAMM* and *L1CAM2* genes; as well as the biallelic loss of the *p16INK4A/CDKN2A* gene are illustrated (Fig. 4D).

Discussion

This is the first comprehensive study of high-resolution DNA copy number analysis in a multitude of genes in NF1 tumor samples. The main aim of the study was to compare the DNA dosage of 57 selected genes and identify key alterations that

possibly underlie the progression of benign NF1 tumors to malignancy.

It is known that patterns of gene copy number alterations can be identified, which are specific to benign, premalignant, and malignant states (19, 20). However, to our knowledge, there are no reports that have done a parallel high-resolution analysis of amplifications and deletions in NF1 tumors. We constructed a microarray that covered 57 selected genes, the majority of which have been suggested to be important in MPNST development by previous expression studies (1, 5, 7–14). In addition, we have also included a set of genes known to be relevant to cancer (*KRAS*, *FOS*, *JUN*, and *TP73*), cell cycle regulation (*CCND1*, *CCNE2*, *CDKN1A*, and *CDKN1B*), and genes involved in the mammalian target of rapamycin pathway (*TSC1*, *TSC2*, *PTEN*, and *mTOR*; ref. 26).

MPNST-specific copy number alterations were identified in 47 genes (82%) studied on this array. Deletions were more frequent than amplifications in MPNSTs, which is in agreement with the earlier CGH studies (15, 27). Moreover, this microarray study substantiates our previous observation that it is the loss of *NF1* gene, as evidenced by loss of heterozygosity that is a common somatic mutation in MPNSTs but is not a predominant germline mutation (28).

Although previous investigations in MPNSTs have presented aberrations from 5q33, 11q22, and 17q25 (16, 17, 27), harboring *HMMR*, *MMP13*, and *ITGB4* genes, respectively, this study reports the involvement of specific genes from these loci. Hemizygous deletion of the *HMMR/RHAMM* gene, coding for Rhamm (a hyaluronan binding protein), was observed in 46% of the MPNSTs. The *HMMR/RHAMM* gene is a major cell cycle–regulated gene (29) involved in Ras signaling (30) and controlling the expression of mitogen-activated protein kinase (31). Overexpression of Rhamm has been implicated in various types of cancer (32–34), including NF1-associated MPNSTs (5). However, the copy number status of *HMMR/RHAMM* in cancer conditions is largely unknown. The identification of *HMMR/RHAMM* deletions, specifically in MPNSTs, in this study advocates it as a strong candidate for initiation and/or development of malignancy in NF1 individuals.

Deletion of the *MMP13* gene was also observed in 43% of the MPNST series. It is known that an imbalance in matrix metalloproteinase and tissue metallopeptidase inhibitors may contribute to malignant phenotype (35, 36). Thus, our data for the *MMP13*, *MMP9*, and *TIMP4* genes (Table 1) indicate that alterations in these genes may confer growth advantage to malignant cells.

The *ITGB4* gene was found to be amplified in 32% of MPNSTs. Integrins are transmembrane receptors that mediate cell-matrix or cell-cell adhesion, and transduce signals that regulate gene expression and cell growth, including Schwann cells. Altered expression of the *ITGB4* has been shown in schwannomas (37) and MPNSTs (5). Therefore, it is likely that the amplification of *ITGB4* gene provides growth advantage to the Schwann cells in malignant tumors.

The identification of concomitant aberrations in the *HGF*, *MET*, and *PDGFRA* genes in MPNSTs is an intriguing observation. The HGF-MET system has been implicated in mitogenesis in cancer (38), including NF1 tumors (39, 40). Moreover, there is evidence that the HGF-PDGFRA-p70S6K pathway plays an essential role during tumor angiogenesis, and rapamycin limits tumor growth through inhibition of p70S6K (41). A recent study has also reported mammalian target of rapamycin and p70S6K1 signaling in prostate cancer cells (42). In view of our data and these studies, we propose that the overrepresentation of *HGF*, *MET*, and *PDGFRA* genes is directly linked to MPNST tumorigenesis and is not an incidental finding. Therefore, it is possible that therapy directed to blocking the p70S6K pathway might be a useful approach for the treatment of MPNSTs.

We also identified amplifications of two genes involved in apoptosis, namely *BIRC5/Survivin* (25% cases) and *TP73* (14% cases). Survivin is an inhibitor of apoptosis, and the up-regulation of *BIRC5* is a frequent alteration in several human cancers, including MPNSTs (5, 14, 18, 43, 44). Similarly, amplification of the *TP73* gene in MPNSTs implies that it is likely that the ΔNp73 protein, an inhibitor of apoptosis (45), is overrepresented in malignant Schwann cells. Deletion of *p16INK4A/CDKN2A*, *RB1*, and *TP53* genes in MPNSTs (Tables 1 and 2) corroborate the model of coinactivation of the *NF1*, *TP53*, and/or *RB1* pathways with functional consequences on cell growth control and apoptosis (1, 6, 46–49).

For the majority of the aberrant genes, there is an agreement between copy number changes observed by the MPNST microarray and the expression data from previous studies. For instance, amplification of *BIRC5*, *CCNE2*, *FOXA2*, *MMP9*, *SOX10*, *SPP1*, *TERT*, and *TP73* correlates with the up-regulation of these genes (5). Similarly, deletions of *L1CAM2*, *PTCH2*, *RB1*, and *TIMP4* agree with previous data, which report down-regulation of these genes in MPNSTs (5, 46).

In benign neurofibromas, the majority of the analyzed genes displayed diploid ratios, indicating that the *NF1* gene mutation in Schwann cells may be sufficient for transforming cells to neurofibromas. These data substantiates that gross chromosomal aberrations are not common in benign neurofibromas (50).

The MPNST-specific alterations in the *HMMR/RHAMM*, *MMP13*, *p16INK4A/CDKN2A*, *ITGB4*, *HGF*, *MET*, and *PDGFRA* genes identified in this study call for further investigations of their putative role in initiation and/or progression of malignancy in NF1 patients. Subsequent to the design of this study, a few other genes have been suggested to be important in MPNSTs such as the *TWIST1* (1), *TNC* (14, 51), *TRIO*, *NKD2*, and *IRX2* (52). These genes could be added to further versions of the MPNST array. In fact, the coverage of this array can be expanded to all the cancer-related genes (53).

It is an exciting prospect that a single "cancer chip" can be used for copy number analysis of DNA derived from cancer at different stages. This should provide vital information regarding the biological and genetic progression of benign NF1 tumors to malignant stages. Moreover, analysis of different types of cancer using this same microarray platform should elucidate the alterations that can transform cells into a tumorigenic state. Such analysis could also be done using BAC clone–based (54) or oligonucleotide microarrays (NimbleGen Systems; Agilent Technologies) spanning the entire human genome. However, when compared with the exon-level arrays, these platforms are limited by one or more factors such as cost, availability, and resolution of analysis.

Because our MPNST microarray has been constructed by spotting the exonic sequences from cancer-specific genes, it is possible to profile gene expression using the same array. Promoter sequences from these genes may also be appended to the existing array design, allowing the analysis of methylation patterns in tumor tissue. This single microarray platform should have the potential to permit the analysis of DNA copy number, gene expression, and epigenetic profiling. Such an approach should have significant effect on our understanding of the cancer genome.

Acknowledgments

We thank the patients for their support, Martin Horan for help in the real-time PCR analysis, and to Ajay Pandita and Rasmussen Kiehl for providing us NF1 tumor samples from the University of Toronto Nervous System Tumour Bank.

References

1. Miller SJ, Rangwala F, Williams J, et al. Large-scale molecular comparison of human schwann cells to malignant peripheral nerve sheath tumor cell lines and tissues. Cancer Res 2006;66:2584–91.
2. Ferner RE, Huson SM, Thomas N, et al. Guidelines for the diagnosis and management of individuals with neurofibromatosis 1. J Med Genet 2007;44:81–8.
3. Evans DG, Baser ME, McGaughran J, Sharif S, Howard E, Moran A. Malignant peripheral nerve sheath tumours in neurofibromatosis 1. J Med Genet 2002;39:311–4.
4. Perry A, Roth KA, Banerjee R, Fuller CE, Gutmann DH. NF1 deletions in S-100 protein-positive and negative cells of sporadic and neurofibromatosis 1 (NF1)-associated plexiform neurofibromas and malignant peripheral nerve sheath tumors. Am J Pathol 2001;159:57–61.
5. Levy P, Vidaud D, Leroy K, et al. Molecular profiling of malignant peripheral nerve sheath tumors associated with neurofibromatosis type 1, based on large-scale real-time RT-PCR. Mol Cancer 2004;3:20.
6. Kourea HP, Orlow I, Scheithauer BW, Cordon-Cardo C, Woodruff JM. Deletions of the INK4A gene occur in malignant peripheral nerve sheath tumors but not in neurofibromas. Am J Pathol 1999;155:1855–60.
7. Holtkamp N, Reuss DE, Atallah I, et al. Subclassification of nerve sheath tumors by gene expression profiling. Brain Pathol 2004;14:258–64.
8. Lee PR, Cohen JE, Tendi EA, et al. Transcriptional profiling in an MPNST-derived cell line and normal human Schwann cells. Neuron Glia Biol 2004;1:135–47.
9. Levy P, Bieche I, Leroy K, et al. Molecular profiles of neurofibromatosis type 1-associated plexiform neurofibromas: identification of a gene expression signature of poor prognosis. Clin Cancer Res 2004;10:3763–71.
10. Watson MA, Perry A, Tihan T, et al. Gene expression profiling reveals unique molecular subtypes of Neurofibromatosis Type I-associated and sporadic malignant peripheral nerve sheath tumors. Brain Pathol 2004;14:297–303.
11. Agesen TH, Florenes VA, Molenaar WM, et al. Expression patterns of cell cycle components in sporadic and neurofibromatosis type 1-related malignant peripheral nerve sheath tumors. J Neuropathol Exp Neurol 2005;64:74–81.
12. Dang I, Nelson JK, DeVries GH. c-Kit receptor expression in normal human Schwann cells and Schwann cell lines derived from neurofibromatosis type 1 tumors. J Neurosci Res 2005;82:465–71.
13. Stonecypher MS, Byer SJ, Grizzle WE, Carroll SL. Activation of the neuregulin-1/ErbB signaling pathway promotes the proliferation of neoplastic Schwann cells in human malignant peripheral nerve sheath tumors. Oncogene 2005;24:5589–605.
14. Karube K, Nabeshima K, Ishiguro M, Harada M, Iwasaki H. cDNA microarray analysis of cancer associated gene expression profiles in malignant peripheral nerve sheath tumours. J Clin Pathol 2006;59:160–5.
15. Lothe RA, Karhu R, Mandahl N, et al. Gain of 17q24-qter detected by comparative genomic hybridization in malignant tumors from patients with von Recklinghausen's neurofibromatosis. Cancer Res 1996;56:4778–81.
16. Schmidt H, Taubert H, Meye A, et al. Gains in chromosomes 7, 8q, 15q and 17q are characteristic changes in malignant but not in benign peripheral nerve sheath tumors from patients with Recklinghausen's disease. Cancer Lett 2000;155:181–90.
17. Bridge RS, Jr., Bridge JA, Neff JR, Naumann S, Althof P, Bruch LA. Recurrent chromosomal imbalances and structurally abnormal breakpoints within complex karyotypes of malignant peripheral nerve sheath tumour and malignant triton tumour: a cytogenetic and molecular cytogenetic study. J Clin Pathol 2004;57:1172–8.
18. Storlazzi C, Brekke H, Mandahl N, et al. Identification of a novel amplicon at distal 17q containing the BIRC5/SURVIVIN gene in malignant peripheral nerve sheath tumours. J Pathol 2006;209:492–500.
19. Nigro JM, Misra A, Zhang L, et al. Integrated array-comparative genomic hybridization and expression array profiles identify clinically relevant molecular subtypes of glioblastoma. Cancer Res 2005;65:1678–86.
20. Yi Y, Mirosevich J, Shyr Y, Matusik R, George AL, Jr. Coupled analysis of gene expression and chromosomal location. Genomics 2005;85:401–12.
21. Mantripragada KK, Buckley PG, Jarbo C, Menzel U, Dumanski JP. Development of NF2 gene specific, strictly sequence defined diagnostic microarray for deletion detection. J Mol Med 2003;81:443–51.
22. Mantripragada KK, Thuresson AC, Piotrowski A, et al. Identification of novel deletion breakpoints bordered by segmental duplications in the NF1 locus using high resolution array-CGH. J Med Genet 2006;43:28–38.
23. Jhanwar SC, Chen Q, Li FP, Brennan MF, Woodruff JM. Cytogenetic analysis of soft tissue sarcomas. Recurrent chromosome abnormalities in malignant peripheral nerve sheath tumors (MPNST). Cancer Genet Cytogenet 1994;78:138–44.
24. De Raedt T, Brems H, Wolkenstein P, et al. Elevated risk for MPNST in NF1 microdeletion patients. Am J Hum Genet 2003;72:1288–92.
25. Spurlock G, Griffiths S, Uff J, Upadhyaya M. Somatic alterations of the NF1 gene in an NF1 individual with multiple benign tumours (internal and external) and malignant tumour types. Fam Cancer 2007;6:463–71.
26. Johannessen CM, Reczek EE, James MF, Brems H, Legius E, Cichowski K. The NF1 tumor suppressor critically regulates TSC2 and mTOR. Proc Natl Acad Sci U S A 2005;102:8573–8.
27. Koga T, Iwasaki H, Ishiguro M, Matsuzaki A, Kikuchi M. Losses in chromosomes 17, 19, and 22q in neurofibromatosis type 1 and sporadic neurofibromas: a comparative genomic hybridization analysis. Cancer Genet Cytogenet 2002;136:113–20.
28. Upadhyaya M, Kluwe L, Spurlock G, et al. The germline and somatic NF1 gene mutation spectrum in NF1-associated malignant peripheral nerve sheath tumours (MPNST). Hum Mutat 2008;29:74–82.
29. Cho RJ, Huang M, Campbell MJ, et al. Transcriptional regulation and function during the human cell cycle. Nat Genet 2001;27:48–54.
30. Hall CL, Yang B, Yang X, et al. Overexpression of the hyaluronan receptor RHAMM is transforming and is also required for H-ras transformation. Cell 1995;82:19–26.
31. Zhang S, Chang MC, Zylka D, Turley S, Harrison R, Turley EA. The hyaluronan receptor RHAMM regulates extracellular-regulated kinase. J Biol Chem 1998;273:11342–8.
32. Maxwell CA, Keats JJ, Belch AR, Pilarski LM, Reiman T. Receptor for hyaluronan-mediated motility correlates with centrosome abnormalities in multiple myeloma and maintains mitotic integrity. Cancer Res 2005;65:850–60.
33. Akiyama Y, Jung S, Salhia B, et al. Hyaluronate receptors mediating glioma cell migration and proliferation. J Neurooncol 2001;53:115–27.
34. Tolg C, Poon R, Fodde R, Turley EA, Alman BA. Genetic deletion of receptor for hyaluronan-mediated motility (Rhamm) attenuates the formation of aggressive fibromatosis (desmoid tumor). Oncogene 2003;22:6873–82.
35. Jiang Y, Goldberg ID, Shi YE. Complex roles of tissue inhibitors of metalloproteinases in cancer. Oncogene 2002;21:2245–52.
36. Stamenkovic I. Matrix metalloproteinases in tumor invasion and metastasis. Semin Cancer Biol 2000;10:415–33.
37. Utermark T, Kaempchen K, Hanemann CO. Pathological adhesion of primary human schwannoma cells is dependent on altered expression of integrins. Brain Pathol 2003;13:352–63.
38. Peruzzi B, Bottaro DP. Targeting the c-Met signaling pathway in cancer. Clin Cancer Res 2006;12:3657–60.
39. Krasnoselsky A, Massay MJ, DeFrances MC, Michalopoulos G, Zarnegar R, Ratner N. Hepatocyte growth factor is a mitogen for Schwann cells and is present in neurofibromas. J Neurosci 1994;14:7284–90.
40. Rao UN, Sonmez-Alpan E, Michalopoulos GK. Hepatocyte growth factor and c-MET in benign and malignant peripheral nerve sheath tumors. Hum Pathol 1997;28:1066–70.
41. Tsutsumi N, Yonemitsu Y, Shikada Y, et al. Essential role of PDGFRα-p70S6K signaling in mesenchymal cells during therapeutic and tumor angiogenesis *in vivo*: role of PDGFRα during angiogenesis. Circ Res 2004;94:1186–94.
42. Vaira V, Lee CW, Goel HL, Bosari S, Languino LR, Altieri DC. Regulation of survivin expression by IGF-1/mTOR signaling. Oncogene 2007;26:2678–84.
43. Wurl P, Kappler M, Meye A, et al. Co-expression of survivin and TERT and risk of tumour-related death in patients with soft-tissue sarcoma. Lancet 2002;359:943–5.
44. Altieri DC. Validating survivin as a cancer therapeutic target. Nat Rev Cancer 2003;3:46–54.
45. Melino G, De Laurenzi V, Vousden KH. p73: friend or foe in tumorigenesis. Nat Rev Cancer 2002;2:605–15.
46. Mawrin C, Kirches E, Boltze C, Dietzmann K, Roessner A, Schneider-Stock R. Immunohistochemical and molecular analysis of p53, RB, and PTEN in malignant peripheral nerve sheath tumors. Virchows Arch 2002;440:610–5.
47. Perrone F, Tabano S, Colombo F, et al. p15INK4b, p14ARF, and p16INK4a inactivation in sporadic and neurofibromatosis type 1-related malignant peripheral

nerve sheath tumors. Clin Cancer Res 2003;9:4132–8.
48. Zhou H, Coffin CM, Perkins SL, Tripp SR, Liew M, Viskochil DH. Malignant peripheral nerve sheath tumor: a comparison of grade, immunophenotype, and cell cycle/growth activation marker expression in sporadic and neurofibromatosis 1-related lesions. Am J Surg Pathol 2003;27:1337–45.
49. Carroll SL, Stonecypher MS. Tumor suppressor mutations and growth factor signaling in the pathogenesis of NF1-associated peripheral nerve sheath tumors: II. The role of dysregulated growth factor signaling. J Neuropathol Exp Neurol 2005;64:1–9.
50. Mertens F, Dal Cin P, De Wever I, et al. Cytogenetic characterization of peripheral nerve sheath tumours: a report of the CHAMP study group. J Pathol 2000;190:31–8.
51. Levy P, Ripoche H, Laurendeau I, et al. Microarray-based identification of tenascin C and tenascin XB, genes possibly involved in tumorigenesis associated with neurofibromatosis type 1. Clin Cancer Res 2007;13:398–407.
52. Adamowicz M, Radlwimmer B, Rieker RJ, et al. Frequent amplifications and abundant expression of TRIO, NKD2, and IRX2 in soft tissue sarcomas. Genes Chromosomes Cancer 2006;45:829–38.
53. Futreal PA, Coin L, Marshall M, et al. A census of human cancer genes. Nat Rev Cancer 2004;4:177–83.
54. Ishkanian AS, Malloff CA, Watson SK, et al. A tiling resolution DNA microarray with complete coverage of the human genome. Nat Genet 2004;36:299–303.

Clinical Cancer Research

High-Resolution DNA Copy Number Profiling of Malignant Peripheral Nerve Sheath Tumors Using Targeted Microarray-Based Comparative Genomic Hybridization

Kiran K. Mantripragada, Gillian Spurlock, Lan Kluwe, et al.

Clin Cancer Res 2008;14:1015-1024.